

Supplementary Information

Cation enrichment in the ion atmosphere is promoted by local hydration of DNA

Chun Yu Ma¹, Simone Pezzotti¹, Gerhard Schwaab¹, Magdalena Gebala², Dan Herschlag² and Martina Havenith^{1,*}.

¹ Department of Physical Chemistry II, Ruhr-University Bochum, 44780 Bochum, Germany.

² Department of Biochemistry, Stanford University, Stanford, California 94305, United States.

* Corresponding Author: martina.havenith@rub.de

THz measurements

We recorded the absorption spectrum of five different bulk electrolytes (CsF, CsCl, KCl, NaF, NaCl) as sample solutions, prepared as described in the main text. . All measurements were carried out at 20°C using a Vertex 80v commercial Fourier Transform infrared (FTIR) spectrometer from Bruker Co. (USA) with a spectral range of 30 to 650 cm⁻¹ and a resolution of 0.5 cm⁻¹. THz/FIR absorption coefficients are obtained from the Lambert-Beer Law:

$$\alpha(\tilde{\nu})_{\text{sample}} = -\frac{1}{d} \ln \left(\frac{I_{\text{sample}}}{I_{\text{ref}}} \right) + \alpha(\tilde{\nu})_{\text{ref}} \quad (\text{S1})$$

Here, $\alpha(\tilde{\nu})_{\text{sample}}$ is the absorption coefficient of the sample solution, and d is the sample thickness. I_{sample} and I_{ref} are the transmitted light intensities containing either the sample or a reference sample with a well-known absorption coefficient $\alpha(\tilde{\nu})_{\text{ref}}$, respectively. To minimize etalon effects, we used water as the reference, which has nearly the same index of refraction as the investigated solutions. For all dsDNA electrolyte mixtures, the corresponding 0.5 M bulk electrolyte solutions were used as the reference.

The reference THz/FIR absorption coefficient of bulk water at a temperature of 20 °C was obtained using temperature-dependent absorption measurements performed in our lab. These were referenced to water data at 25 °C by Bertie and Lan.¹ We used the following model to describe the water spectrum:

(S2)

α_{bw}

$$= \sum_{i=1}^2 \frac{a_i \exp\left(-\frac{\tilde{\nu}}{\tilde{\nu}_i}\right)}{\left(\tilde{\nu}^2 + \frac{\omega_i^2}{\pi^2}\right)} \tilde{\nu}^2 + \sum_{i=3}^5 \frac{a_i * \frac{\omega_i^2}{\pi^2} \tilde{\nu}^2 \exp\left[-\frac{\tilde{\nu}}{\tilde{\nu}_{co,i}}\right]}{4\pi^3 \left[\tilde{\nu}_{d,i}^2 + \frac{\omega_i^2 \exp\left[-\frac{\tilde{\nu}}{\tilde{\nu}_{co,i}}\right]}{4\pi^2} - \right]}$$

Here the first two terms describe the low-frequency Debye-like relaxations. The next three terms are attributed to damped harmonic oscillations originating from the intermolecular hydrogen bond stretch and two librational motions of water. The results of the fit are summarized in Table S1.

Table S1. Fit parameters of the water model at 20 °C.

Mode	Amplitude, a_i	Center Frequency, $\tilde{\nu}_i$	Width, ω_i	Cutoff Freq, $\tilde{\nu}_{co,i}$
1	78.71 cm ⁻¹	-	3.14 cm ⁻¹	205.18 cm ⁻¹
2	177.98 cm ⁻¹	-	49.18 cm ⁻¹	205.18 cm ⁻¹
3	730.05 cm ⁻¹	146.37 cm ⁻¹	1495.25 cm ⁻¹	205.18 cm ⁻¹
4	2796.08 cm ⁻¹	572.13 cm ⁻¹	4835.61 cm ⁻¹	619.71 cm ⁻¹
5	1252.62 cm ⁻¹	768.04 cm ⁻¹	8153.45 cm ⁻¹	334.46 cm ⁻¹

The absorption coefficient, α_{bw} , of bulk water can be described by the product of water concentration, C_{bw} , and the molar extinction coefficient of water, ϵ_{bw} :

$$\alpha_{bw} = C_{bw} \epsilon_{bw} \quad (S3)$$

Absorption spectra of bulk electrolytes

Using a combination of THz/FIR spectroscopy and *ab initio* molecular dynamics simulations we have demonstrated in a previous work³ that the changes of the THz spectrum of solvated ions compared to bulk water is dominated by the dipolar auto- and cross-correlations of the ion with the first and second hydration shell. At concentrations up to 1 M, we can neglect cooperativity effects between the hydrated anions and cations (see Figure 1). Based upon this model, the absorption coefficient of a bulk electrolyte solution, $\alpha_{be}(\tilde{\nu})$, can be dissected into a superposition of a bulk water component and hydrated ion contributions. For 1:1 electrolytes,

the concentration of cations and anions are equal to the salt concentration c_s . Assuming additivity, we obtain:

$$\alpha_{be}(\tilde{\nu}) = c_s(\varepsilon_M^{be} + n_{h,M}^{be}\varepsilon_{h,M}^{be}) + c_s(\varepsilon_X^{be} + n_{h,X}^{be}\varepsilon_{h,X}^{be}) + c_{bw}^{be}\varepsilon_{bw} \quad (\text{S4})$$

Here, M and X denote cation and anion, respectively, and $n_{h,\Gamma}^{be}$ ($\Gamma = M, X$) the hydration number of the corresponding ion. c_s and c_{bw}^{be} are the salt and bulk water concentrations in the electrolyte, respectively. ε_{bw} is the molar extinction coefficient of bulk water. The extinction coefficients of cations and anions are $\varepsilon_{\Gamma}^{be}$ ($\Gamma = M, X$), the hydration water is described by $\varepsilon_{h,\Gamma}^{be}$ ($\Gamma = M, X$).²

Please note, that these are volume averages of a bulk solution. Based on these assumptions, the hydration numbers and hydration water extinctions are effective values that can be determined from concentration dependent THz absorption measurements (see ref.²).

The sum of hydration water and bulk water is equal to the total amount of water in the solution, c_w^{be} :

$$c_w^{be} = c_s(n_{h,M}^{be} + n_{h,X}^{be}) + c_{bw}^{be} \quad (\text{S5})$$

In our previous work, the effective ionic absorption coefficient, $\alpha_{ion}^{eff}(\tilde{\nu})$, was defined as:³

$$\alpha_{ion}^{eff}(\tilde{\nu}) = \alpha_{be} - c_w^{be}\varepsilon_{bw} \quad (\text{S6})$$

Combining Equations S4, S5, and S6 yields:

$$\alpha_{ion}^{eff}(\tilde{\nu}) = c_s(\varepsilon_M^{be} + n_{h,M}^{be}\varepsilon_{h,M}^{be}) + c_s(\varepsilon_X^{be} + n_{h,X}^{be}\varepsilon_{h,X}^{be}) - c_s(n_{h,M}^{be} + n_{h,X}^{be})\varepsilon_{bw} \quad (\text{S7})$$

$$= c_s(\varepsilon_M^{be} + \varepsilon_X^{be}) + c_s n_{h,M}^{be}(\varepsilon_{h,M}^{be} - \varepsilon_{bw}) + c_s n_{h,X}^{be}(\varepsilon_{h,X}^{be} - \varepsilon_{bw}) \quad (\text{S8})$$

In Equation S8, $\alpha_{ion}^{eff}(\tilde{\nu})$ is directly proportional to salt concentration. This is confirmed experimentally for the concentration range used in this study. In the main text, we used the effective molar ionic extinction coefficient ε_{ion}^{eff} which is defined as:

$$\varepsilon_{ion}^{eff}(\tilde{\nu}) = \frac{\alpha_{ion}^{eff}(\tilde{\nu})}{c_s} = [\varepsilon_M^{be} + n_{h,M}^{be}(\varepsilon_{h,M}^{be} - \varepsilon_{bw})] + [\varepsilon_X^{be} + n_{h,X}^{be}(\varepsilon_{h,X}^{be} - \varepsilon_{bw})] \quad (\text{S9})$$

According to Equation S9, the spectra can be dissected into a sum of ionic extinctions, i.e. rattling modes, plus the total changes of the water extinctions given by the presence of the

ions, i.e. by the sum of the product of $n_{h,\Gamma}^{be}$ and the difference of the extinction coefficients between hydration water and bulk water, $(\epsilon_{h,\Gamma}^{be} - \epsilon_{bw})$, averaged over the over the probe volume.

In Figure S1 we plot α_{be} and α_{ion}^{eff} of 0.5 M NaCl in water as an example. α_{bw} of bulk water is included for comparison. ϵ_{ion}^{eff} of all other salt solutions is shown in Figure S2.

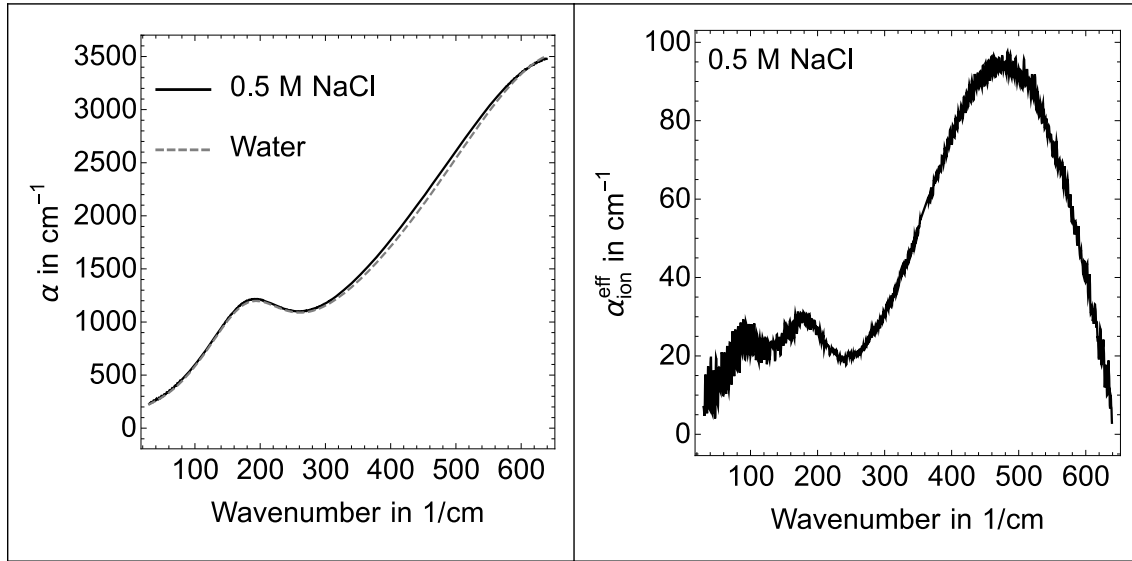


Figure S1. Left: Total absorption of bulk electrolyte, α_{be} (black), and bulk water, α_{bw} (dashed red). Right: Effective absorption coefficient, α_{ion}^{eff} of 0.5 M NaCl after subtraction of the concentration scaled absorption coefficient of bulk water (black).

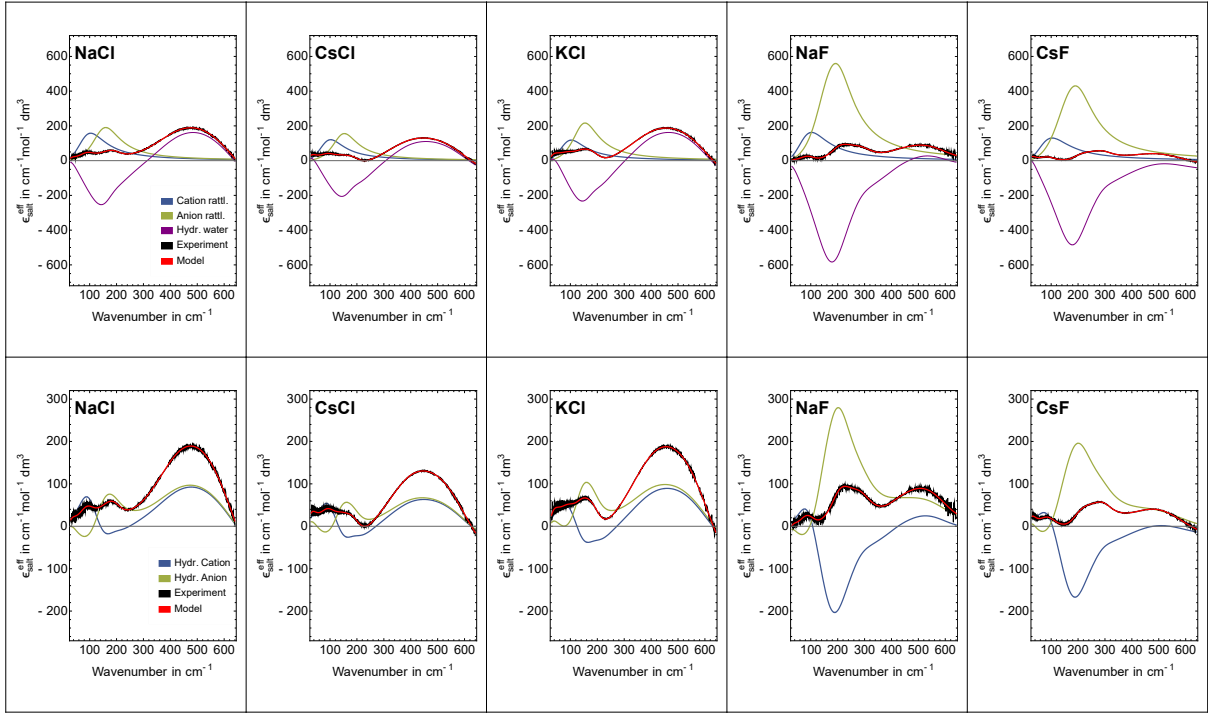


Figure S2. Top: molar extinction coefficients ϵ_{ion}^{eff} of the different electrolytes and their dissection in cation rattling (blue), anion rattling (green) and hydration water (purple) contributions (see text for details). Bottom: Dissection of ϵ_{ion}^{eff} into hydrated cationic and anionic contributions assuming the hydration water effect is equally shared between the ions.

Spectral dissection of the effective ionic extinction coefficient of bulk electrolytes

Heuristically, we found that the observed ionic and hydration water modes can be described with a minimum number of fitting parameters (Ockham's razor) using damped harmonic oscillators (DHO):

$$L_i(\tilde{\nu}, a_i, \omega_i, \tilde{\nu}_{d,i}) = \frac{a_i * \omega_i^2 \tilde{\nu}^2}{4\pi^2 \left[\left(\tilde{\nu}_{d,i}^2 + \frac{\omega_i^2}{4\pi^2} - \tilde{\nu}^2 \right)^2 + \frac{\omega_i^2}{\pi^2} \tilde{\nu}^2 \right]} \quad (\text{S10})$$

with amplitude a_i , damping width ω_i , and damped center frequency $\nu_{d,i}$. The low-frequency region ($\tilde{\nu} < 50 \text{ cm}^{-1}$) is difficult to fit and approximated by a damped harmonic oscillator function with $\tilde{\nu}_d = 0 \text{ cm}^{-1}$. Describing the ionic and hydration water modes as damped harmonic oscillators, Equation S9 yields:

$$\varepsilon_{ion}^{eff} \approx n_h \left[\sum_{i=1}^n L_i(\tilde{\nu}, a_i, \omega_i, \tilde{\nu}_{d,i}) - \varepsilon_{bw} \right] \quad (S11)$$

$n_h = n_{h,M}^{be} + n_{h,X}^{be}$ denotes the effective spectroscopic hydration shell size per mole of salt. n_h is difficult to determine and strongly correlates with the amplitudes a_i of the damped harmonic oscillators. To determine these amplitudes more precisely, we therefore normalized all oscillator strengths to n_h (see Equation S11 and Tables S2-S3). For all electrolytes discussed here, ε_{ion}^{eff} can be decomposed into the cation contribution $\varepsilon_M^{be}(\tilde{\nu})$, the anion contribution $\varepsilon_X^{be}(\tilde{\nu})$, and the difference of the hydration water bands and the bulk water absorption coefficient:

$$\varepsilon_{ion}^{eff} = \varepsilon_M^{be}(\tilde{\nu}) + \varepsilon_X^{be}(\tilde{\nu}) + n_h \{ \varepsilon_{hw}^{be} - \varepsilon_{bw} \} \quad (S12)$$

where ε_M^{be} (one DHO) and ε_X^{be} (one DHO for Cl⁻, two DHOs for F⁻) represent the molar extinction coefficients attributed to rattling mode(s) of cation and anion, respectively, while ε_{hw}^{be} (four DHOs) describes the hydration water contributions.

In Figure S2, top, we display the measured extinction coefficients of the five electrolytes (black), and compare this to the reconstructed spectra (red). In addition, we show the dissection of ε_{ion}^{eff} into the cationic, anionic and hydration water contributions. In Figure S2, bottom, we display the same data together with the estimates of the hydrated cation and hydrated anion contributions. In order to estimate these, we needed to use a further assumption. Here, we assumed that the hydration water response is equally shared between the anion and the cation. For all electrolytes, we observe a cationic rattling mode centered at 70- 90 cm⁻¹. Cl⁻ has a rattling mode centered at 180 cm⁻¹ and F⁻ at 190 and 290 cm⁻¹. Hydration water modes are described by damped harmonic oscillators with center frequencies at 0 cm⁻¹ (Debye-type), at 140 - 150 cm⁻¹ (interface-like), at 370-430 cm⁻¹ (libration 1) and at 570-650 cm⁻¹ (libration 2). The results of the fit are summarized in Tables S2 and S3. Unless specified, errors correspond to a 95% confidence interval.

Table S2: Fit parameters for cationic and anionic damped harmonic oscillator modes. Please note that the amplitudes are normalized to spectroscopic hydration shell size n_h to reduce correlation effects in the fit between distinct fitting parameters. Errors represent the 95% confidence interval.

	Cation Rattl.			Anion Rattl. 1			Anion Rattl. 2		
	ν	A	w	ν	A	w	ν	A	w
NaCl	81.8 \pm 2.3	5.1 \pm 0.6	402. \pm 12.	182.0 \pm 2.0	9.8 \pm 0.8	402. \pm 12.	N/A	N/A	N/A
CsCl	84.5 \pm 3.4	4.8 \pm 0.8	363. \pm 43.	180.8 \pm 1.3	9.1 \pm 0.4	363. \pm 43.	N/A	N/A	N/A
KCl	84. \pm 4.	3.94 \pm 0.35	376. \pm 31.	179.5 \pm 1.6	9.1 \pm 0.6	376. \pm 31.	N/A	N/A	N/A
CsF	73.7 \pm 2.2	4.34 \pm 0.34	460. \pm 9.	187.1 \pm 3.2	9.2 \pm 0.6	460. \pm 9.	290.9 \pm 1.9	0.80 \pm 0.33	288. \pm 35.
NaF	76.8 \pm 3.3	4.47 \pm 0.19	432. \pm 17.	192.2 \pm 3.0	9.5 \pm 0.6	432. \pm 17.	286. \pm 4.	0.92 \pm 0.31	331. \pm 77.

Table S3: Fit parameters for n_h and damped harmonic oscillator modes related to water. Please note that the amplitudes are normalized to spectroscopic hydration shell size n_h to reduce correlation effects in the fit between distinct fitting parameters. Errors represent the 95% confidence interval.

	n_h	Debye		Interface Water			Libration Band 1			Libration Band 2		
		A	w	ν	A	w	ν	A	w	ν	A	w
NaCl	31. \pm 12.	3.56 \pm 0.18	213. \pm 7.	146. \pm 4.	6.1 \pm 0.8	402. \pm 12.	407. \pm 8.	11.7 \pm 3.2	1291. \pm 97.	595. \pm 11.	55.6 \pm 2.5	1721. \pm 76.
CsCl	25. \pm 14.	4.5 \pm 0.8	213. \pm 6.	142.0 \pm 2.2	6.2 \pm 0.5	363. \pm 43.	373.9 \pm 2.0	5.9 \pm 1.0	1002. \pm 156.	578. \pm 26.	59.8 \pm 0.6	1992. \pm 63.
KCl	30. \pm 14.	4.4 \pm 0.7	253. \pm 17.	142.2 \pm 2.6	7.2 \pm 0.8	376. \pm 31.	381.7 \pm 2.5	6.5 \pm 1.2	1014. \pm 119.	574. \pm 22.	59.3 \pm 0.8	1918. \pm 44.
CsF	30. \pm 7.	3.73 \pm 0.19	183. \pm 6.	146. \pm 4.	6.0 \pm 0.6	460. \pm 9.	477. \pm 57.	23. \pm 17.	1966. \pm 268.	643. \pm 21.	42. \pm 18.	1661. \pm 231.
NaF	36. \pm 5.	3.04 \pm 0.07	206. \pm 10.	150.5 \pm 3.1	6.9 \pm 0.7	432. \pm 17.	423. \pm 11.	0.34 \pm 0.35	424. \pm 263.	587.2 \pm 3.2	63.76 \pm 0.17	2104. \pm 35.

Estimation of systematic errors

Estimation of errors is based on a systematic concentration dependent NaCl solutions from two different measurement days (see Figure S3). The solutions were prepared in the concentration range 0.3-1.2M. A singular value decomposition shows that the observed effective absorption coefficient depends linearly on the concentration in the full range (Fig. S3c). A single principal component is sufficient to reproduce the observed spectroscopic changes (Fig. S3b). A comparison between the measured absorption coefficients and those modelled from a linear fit of the scores of the first principal component leads to estimated errors in α_{be}^{eff} of $\delta\alpha_{be}^{eff} \approx \pm 5 \text{ cm}^{-1}$ for frequencies below 100 cm^{-1} in the region of the cationic rattling modes and $\delta\alpha_{be}^{eff} \approx \pm 10 \text{ cm}^{-1}$ for higher frequencies. For $\alpha_{DNA+cloud}^{eff}$ we expect slightly larger errors due to the uncertainty in

the dsDNA volume. Since $\varepsilon_{DNA+cloud}^{eff} = \frac{\alpha_{DNA+cloud}^{eff}}{c_{DNA}}$ the expected error $\delta\varepsilon_{DNA+cloud}^{eff} = \frac{\delta\alpha_{DNA+cloud}^{eff}}{c_{DNA}}$. If we include the uncertainty in the determination of the dsDNA concentration, this leads to a conservative estimate of $\delta\varepsilon_{DNA+cloud}^{eff} \approx \pm 2 \text{ cm}^{-1}$ in the frequency range of the cationic rattling modes, i.e. below 100 cm^{-1} and $\delta\varepsilon_{DNA+cloud}^{eff} \approx \pm 4 \text{ cm}^{-1}$ for higher frequencies.

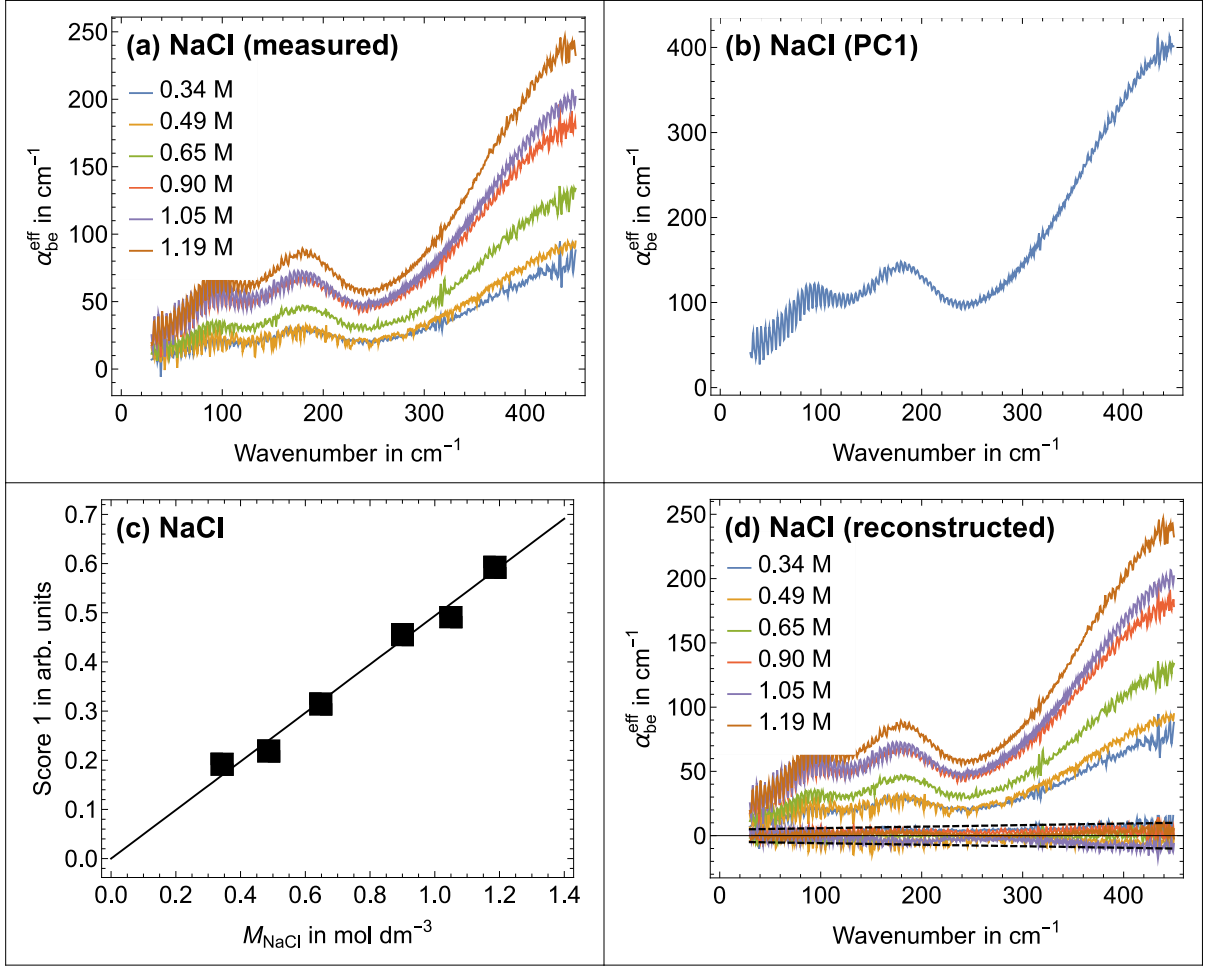


Figure 3: (a) measurements of NaCl aqueous solutions in the concentration range 0.3-1.2M. These data were analysed using principal component analysis based on singular value decomposition. A single principle component (b) that depends linearly on concentration (c) is sufficient to reproduce the measurements. (d) Spectra reconstructed from PC1 and the corresponding linear score function together with their residuals (i.e. measured-reconstructed absorption coefficients). The dashed black lines show that the residuals are contained in a region from $\delta\alpha_{be}^{eff} \approx \pm 5 \text{ cm}^{-1}$ at 30 cm^{-1} to $\delta\alpha_{be}^{eff} \approx \pm 10 \text{ cm}^{-1}$ at 450 cm^{-1} .

Estimation of the molar volume of dsDNA

In order to quantify the dilution due to volume exclusion by dsDNA, we need to know the number of dsDNA in the solution as well as the volume of a single dsDNA molecule. The total number, N_{DNA} , of dsDNA in 100 μL of a 1 mM solution is given by:

$$N_{\text{DNA}} = \left(1 * \frac{10^{-3} \text{ mol}}{1 \text{ dm}^3} \right) * 6.022 * 10^{23} \text{ molecules/mol} * (100 * 10^{-6} \text{ dm}^3)$$

$$= 6.02 * 10^{16} \text{ molecules}$$

The volume of dsDNA is estimated as the sum of the atomic volumes of its molecular constituents. The 24-bp dsDNA used in our experiments has the following sequence:

S1: 5' GGT GAC GAG TGA GCT ACT GGG CGG 3' and

S2: 5' CCG CCC AGT AGC TCA CTC GTC ACC3'

The atomic volume of dsDNA is deduced from the reference atomic volumes of its constituents in the crystal phase. For our further analysis we took the average of data obtained with three different methods.⁴ The total volume of dsDNA, V_{DNA} is the sum of the total volumes of the AT base pairs, V_{AT}^{DNA} , CG base pairs, V_{CG}^{DNA} , and sugar and phosphate groups, V_{SP}^{DNA} .

Therefore,

$$\begin{aligned} V_{DNA} &= (V_{AT}^{DNA} + V_{CG}^{DNA} + V_{SP}^{DNA}) \\ &= [(8*273.7+16*263.5+48*172.73) (10^{-10} \text{ m})^3] \\ &= 1.47*10^{-26} \text{ m}^3 \end{aligned}$$

Taking into account the number of molecules in a 1 mM dsDNA solution, the volume ratio of V_{DNA} to the total volume of solution, V_{total} (100 μL) is given by

$$\begin{aligned} \frac{V_{DNA}}{V_{total}} &= \frac{6.02 * 10^{16} * 1.47 * 10^{-26} \text{ m}^3}{100 * 10^{-6} \text{ dm}^3} \\ &= 0.0086 \text{ per mmol of DNA} \end{aligned}$$

For a 0.5 M electrolyte, this volume ratio corresponds to an ion concentration c_{ion} of

$$\begin{aligned} c_{ion} &= 0.0086 * 0.5 \\ &= 4.3 \text{ mM} \end{aligned}$$

Therefore, we estimate that the volume occupied by each mM dsDNA corresponds to 4.3 mM of salts in a 0.5 M electrolyte, i.e. the dilution factor of 1 dsDNA corresponds to 4 cations and 4 anions.

Concentrations of measured dsDNA-electrolyte solutions

In Table S4 we summarize all measurements. For NaCl the concentration of dsDNA was varied to make sure that all spectra scale linearly with dsDNA concentration. For all other electrolytes the concentration was kept constant.

Table S4. Concentrations used for the measurements of dsDNA in alkali halide solutions

Electrolyte	dsDNA concentration (mM)	Salt concentration (M)
NaCl	0	0.3;0.5;0.6;0.9;1.2;1.5
	1.35;1.5;2.5;8	0.5
NaF	0	0.1;0.2;0.3;0.4;0.5;0.6;0.7;0.9
	4;7	0.5
KCl	0	0.5;1.0;1.5;2.0
	4.6	0.5
CsCl	0	0.5;1;2.0
	4.9	0.5
CsF	0	0.4;0.5;0.8;1.0;1.2;1.6;2.0
	3.5	0.5

Theoretical analysis of the ion-clusters formed in the DNA atmosphere from MD simulations of DNA in NaCl and NaF atmospheres

In ref.⁵ the formation of cluster of ions with average total charge of +1 or 0 within the DNA atmosphere was proposed as a possible molecular mechanism to explain the anion-specific enrichment of cations in the DNA atmosphere. As discussed in the main text, both our theoretical and experimental results provide no evidence for enhanced formation of contact ion-pairs within the DNA atmosphere as compared to the bulk for NaCl and NaF electrolytes. Therefore, we hereafter analyze the size and charge of the clusters of ions forming solvent-separated ion-pairs in the DNA atmosphere and in the bulk for NaCl and NaF aqueous solutions. For the ion-clusters analysis, an ion-ion distance cut-off of 6 Å is adopted for defining ion-ion solvent-separated interactions. Other cut-off values in the 5-7 Å range have been tested and provide the same qualitative results as reported hereafter.

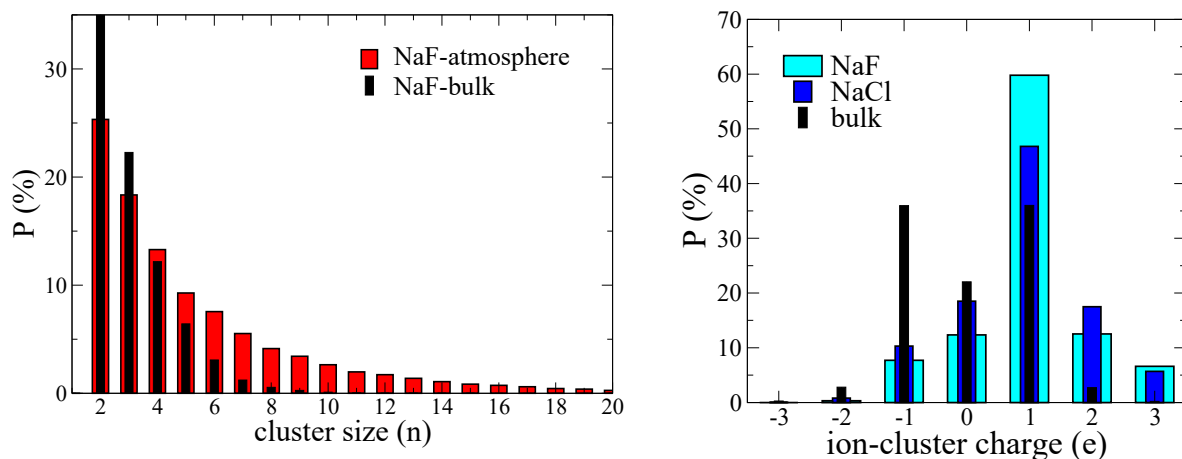


Figure S3. Ion-clusters in the DNA atmosphere Vs bulk. Left: Probability distribution for the size (n being the number of ions, starting from $n=2$) of the clusters formed in the DNA atmosphere (red) and in the bulk (black) for the NaF system. Similar results are obtained for NaCl. The probabilities are normalized so that the sum for all n values greater and equal to 2 is 100%. **Right:** Probability distribution of the charge (in elementary charge) of the ion-clusters in the DNA atmosphere for the NaF (cyan) and NaCl (blue) systems compared to the bulk reference (black). The bulk distribution is presented for NaCl only since NaF provides the same clusters charge distributions in the bulk. For this analysis also ion-clusters made of 1 ion (i.e. single ions) are considered for consistency.

Inspection of the left panel of Figure S3 reveals that, in the case of NaF, both cluster-size distributions in the DNA atmosphere and in the bulk exhibit a monotonic decrease of probability with increasing cluster size (n), suggesting that there is no strong driving force for ion-pairing in the DNA atmosphere as compared to the bulk. However, the decrease is less pronounced in the DNA atmosphere, which can be attributed to ion crowding in this region, in agreement with what was expected from the theoretical and experimental ion-counts. In average, we can therefore conclude that small clusters (with $4 < n < 10$) of ions forming water-mediated interactions are more likely in the DNA atmosphere than in the bulk. A similar conclusion is reached for the NaCl case (data not shown). This result is in agreement with the predictions of ref.⁵.

The analysis of the charge of the clusters provides more remarkable differences between DNA atmosphere and bulk as compared to the cluster-size, as illustrated in the right panel of Figure S3. While in the bulk the charge-distribution is symmetric around the value of 0, as expected, in the cases of both NaCl and NaF DNA atmospheres the most probable total charge of the ion clusters is +1, as one could anticipate due to the negative charge of the DNA substrate,

followed by values of +2 and 0. Again, such distribution is consistent with the propositions of ref.⁵, however it is obtained from our simulations for ions that form solvent-separated and not direct contact ion-pairs.

Theoretical analysis of the hydration layer size and free energy of ion-water interactions for the anions in NaCl and NaF atmospheres.

The first minimum in the $g(r)$ reported in Figure S4, top, defines the size of the 1st hydration shell of the two anions, which has a smaller radius for F^- (~ 3.0 Å) than for Cl^- (~ 3.8 Å). The potential of mean force (PMF) for moving a water molecule from the anion hydration layer to the bulk is directly deduced from the $g(r)$ as $-\ln(g(r))$, and plotted in Figure S4, bottom. The free energy barrier to remove one water molecule from the hydration shell of each of the two anions is estimated as the free energy difference between the 1st minimum and the subsequent maximum in the PMF. The barrier is equal to ~ 4.7 $k_B T$ for F^- , larger than the value of ~ 1.9 $k_B T$ obtained for Cl^- . This result highlights the stronger interaction formed by F^- with its hydration water molecules than Cl^- .

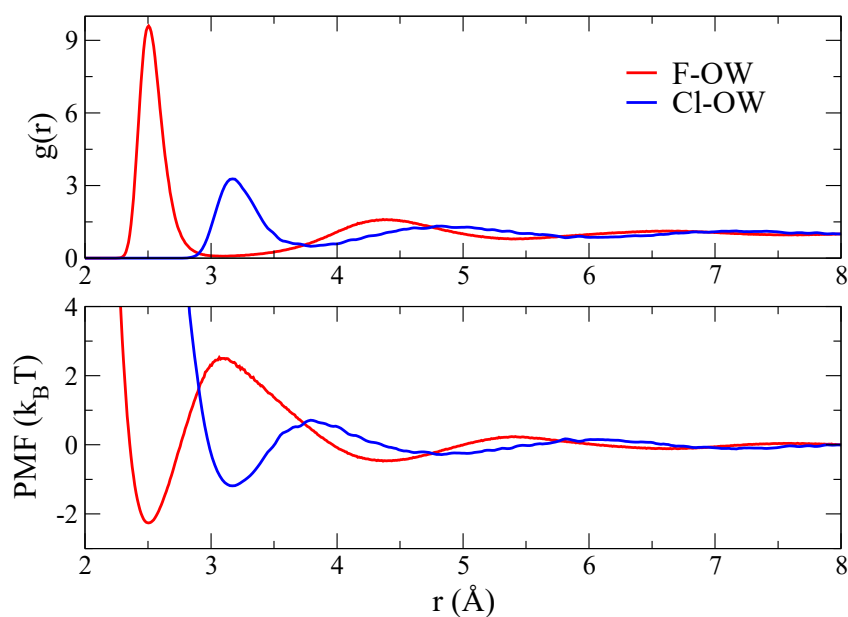


Figure S4. Comparison of anion hydration properties in NaF and NaCl electrolytes. Top: anion-water oxygen atom radial pair distribution function, $g(r)$, for F^- (red) and Cl^- (blue). Corresponding potential of mean force (PMF) for moving a water molecule from the anion hydration layer to the bulk.

References

1. Bertie J. E. and Z. D. Lan, 1996. Infrared intensities of liquids: The intensity of the OH stretching band of liquid water revisited, and the best current values of the optical constants of H₂O(l) at 25 degrees C between 15 000 and 1 cm⁻¹. *Appl. Spectrosc.* **50**, 1047-1057.
2. Schwaab, G., F. Sebastiani, and M. Havenith, 2019. Ion hydration and ion pairing as probed by THz spectroscopy. *Angew. Chem. Int. Ed.* **58**, 3000-3013.
3. Schienbein, P., G. Schwaab, H. Forbert, M. Havenith, and D. Marx, 2017. Correlations in the solute-solvent dynamics reach beyond the first hydration shell of ions. *J. Phys. Chem. Lett.* **8**, 2373-2380.
4. Nadassy, K., I. Toma's-Oliveira, I. Alberts, J. Janin, and S. J. Wodak, 2001. Standard atomic volumes in double-stranded DNA and packing in protein-DNA interfaces. *Nucleic Acids Res.* **29**, 3362-3376.
5. Gebala, M., G. M. Giambaşu, J. Lipfert, N. Bisaria, S. Bonilla, G. Li, D. M. York, and D. Herschlag, 2015. Cation-Anion Interactions within the Nucleic Acid Ion Atmosphere Revealed by Ion Counting. *J. Am. Chem. Soc.* **137**, 14705-14715.